The Evolution of Micromechanical Properties for Zr-Based Metallic Glass Induced by Laser Shock Peening

Yansen Li[1,2], Zhitao Wang[3], Yanpeng Wei[4], Tianyu Chen[2], Chunfeng Zhang[5], Yong Huan[4], Kun Zhang[2]* and Bingchen Wei[2]*

[1]Department of Engineering Mechanics, Shijiazhuang Tiedao University, Shijiazhuang, China, [2]Key Laboratory of Microgravity (National Microgravity Laboratory), Institute of Mechanics, Chinese Academy of Sciences, Beijing, China, [3]Project Management Center of Army Equipment Department, Beijing, China, [4]Institute of Mechanics, Chinese Academy of Sciences, Beijing, China, [5]Taian Changfeng Construction Engineering Project Management Co., Taian, China

The micromechanical properties of Zr-based metallic glass (MG) induced by laser shock peening (LSP) were studied through the use of nanoindentation. The serrations in representative load-displacement (*P-h*) curves exhibited a transformation from stairstep-like to ripple-shaped from untreated zone to shock region, which implied an increase in plastic deformation ability of material after LSP. Significant hardening was also observed in the impact zone, which can be attributed to the effect of compressive residual stress. Both increase in hardness and plastic deformation ability in shock region indicate the excellent effect of LSP on the micromechanical properties of investigated Zr-based MG, which provide a new way to study the deformation mechanism in metallic glasses and a further understanding of plasticization.

Keywords: metallic glass, laser shock peening, nanoindentation, serrations, micromechanical properties

INTRODUCTION

As an attractive material, metallic glasses (MGs) have been extensively investigated during the last decades due to their unique characteristics, such as high yield strength, large elastic deformation, and excellent soft magnetic properties (Inoue, 2000; Wang et al., 2004; Greer and Ma, 2007). However, the plastic deformation of MGs at ambient temperature is usually constrained in a narrow region, namely, the shear band, which generally leads to catastrophic failure of MGs (Greer et al., 2013). The lack of ductility at room temperature greatly hinders the development of MGs for engineering applications.

To improve the plastic deformation ability of MGs, many researchers have paid their attention to the deformation mechanism in MGs. A series of theoretical models for the deformation of such MGs have been proposed, such as free volume model (Spaepen, 1977; Ye et al., 2010), shear transformation zone model (Argon, 1979; Miracle, 2004), and flow units model (Lu et al., 2014; Wang et al., 2014). On the basis of these theoretical studies, a large number of researchers have tried to improve the plasticity of MGs by various methods. For example, Xie and Kruzic (2017) reported that cold rolling could facilitate numerous shear bands along the main crack, which assisted in the fracture toughness of MGs. Zhai et al. (2018) investigated the effect of pre-compression on the microstructures, mechanical properties, and corrosion resistance of Cu-based MG; they found that pre-compression could promote the formation of MG matrix composites to some extent, which induced a certain degree of plasticity. Besides, Di et al. (2020) tried to modify mechanical properties of MG by the way of cryogenic thermal cycling; they made it successful that the plastic strain of FeCoBSiNb MG displayed an obvious improvement and maintained a high yield strength over 4,000 MPa,

FIGURE 1 | Schematic representation of the grid indentation.
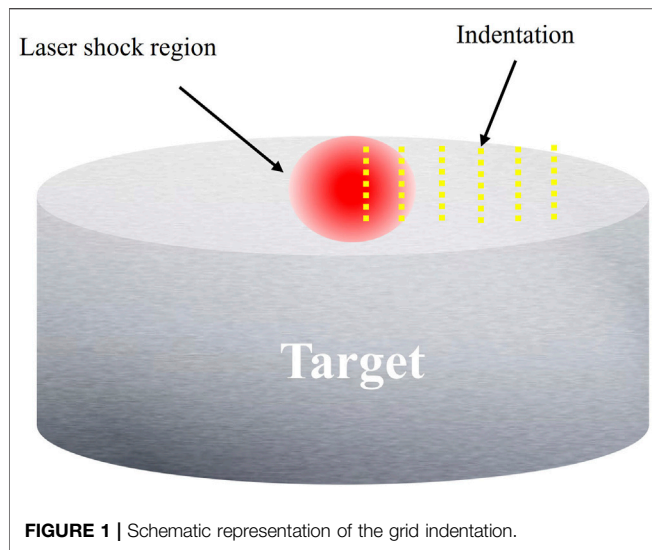
and this excellent performance was attributed to the rejuvenation and fine-tuned crystal-like ordering structures.

Nevertheless, although many methods have been used to improve the plasticity of MGs and the deformation mechanisms have been elucidated to some extent, the mechanical responses of MGs under extreme loading conditions are still not fully understood. Fortunately, laser shock peening (LSP) provides a possible way to explore these responses. LSP is an attractive surface treatment technique (Fabbro et al., 1998; Montross et al., 2002; Liao et al., 2016) with extremely high pressure amplitude (~GPa) within extremely short load time (~ns). The LSP-induced mechanical properties fluctuations may provide a new approach in developing a deeper understanding of the mechanical behavior of MGs.

In this paper, a nanoindentation test was employed to study the micromechanical property evolution of Zr-based MG induced by LSP because it provides an effective method in a controlled manner, typically without the risk of failure in the case of less plasticity (Huang et al., 2016; Liu et al., 2021). The characteristics of nanoindentation curves in different regions of LSP affected zone were analyzed in detail, especially pop-in events. Besides, we also investigated the evolution of microhardness and elastic modulus in this MG after LSP. These results may provide a further understanding of the deformation mechanism in MGs.

MATERIALS AND METHODS

The master alloy of $Zr_{41.2}Ti_{13.8}Cu_{12.5}Ni_{10}Be_{22.5}$ (at%) was prepared by casting method as described in detail in the previous paper of the authors (Li et al., 2019). LSP was performed with a Q-switched Nd: YAG pulse laser. The pulse wavelength and duration were 1,064 nm and 30 ns, respectively. In the LSP experiment, aluminum foil was employed as ablative coating layer (~40 μm). To limit the laser irradiation, purified water was covered on the target. According to the previous works (Xu et al., 2014; Wei et al., 2017), the laser power density was

adjusting to 4 GW/cm². The laser impact spot was anapproximate circle with a diameter of 2.5 mm. The X-ray diffraction test was carried on a Philips PW 1050 diffractometer with Cu Kα radiation. The microstructure observation was conducted on a FEI Tecnai G2 transmission electron microscope.
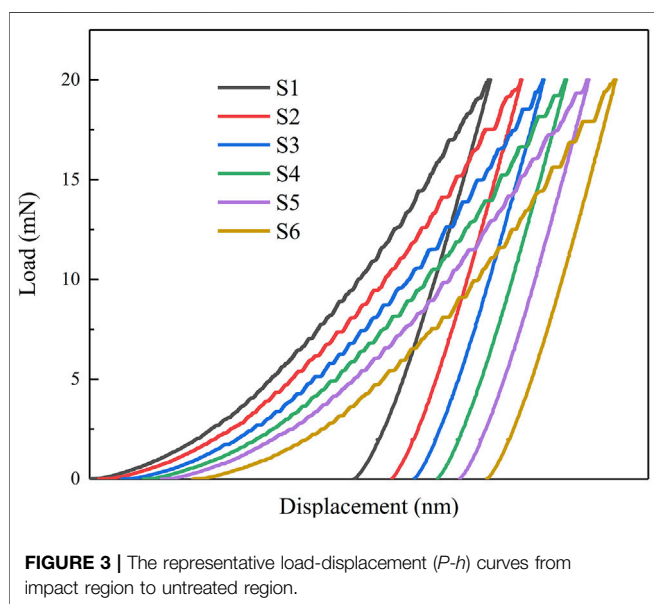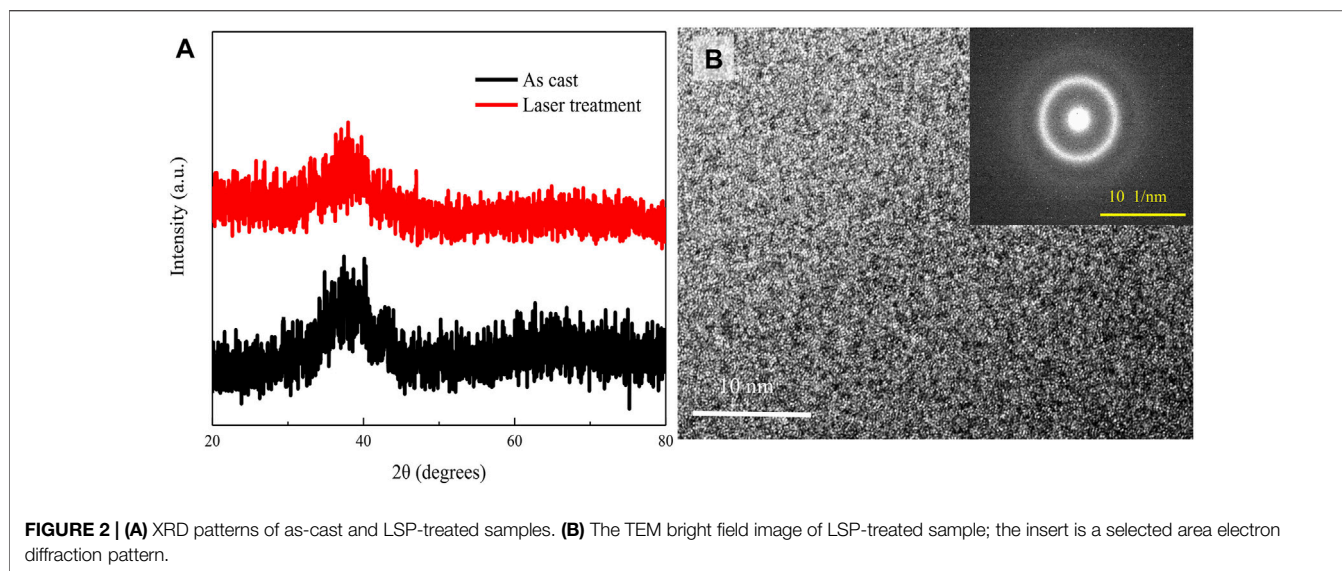
After LSP treatment, the nanoindentation tests were conducted at room temperature using a Nano Indenter G200 with a Berkovich diamond indenter. The indentations were performed in load-controlled mode. The loading rate and maximum loading were 0.05 mN/s and 20 mN, respectively. For the sake of removing the thermal effect, the thermal drift below 0.05 nm/s was maintained. The grid indentation was performed by using an indentation matrix (5 × 6 indents), and the space between each column is 300 μm as illustrated in **Figure 1**.

RESULTS

The XRD patterns of the as-cast and LSP samples are shown in **Figure 2** A. It is evident that only a broad hump can be seen in both XRD patterns, meaning that no crystallization phase exists in these samples. Furthermore, the microstructure of the sample treated by LSP is also examined by TEM. **Figure 2** B displays the TEM bright field image of the LSP-treated sample. It shows no distinct contrast. Besides, a broad diffraction halo was observed in the corresponding selected area electron diffraction. These results proved that the amorphous structure in the LSP-treated sample, which indicated no crystalline grain, was generated during the LSP process.

Figure 3 shows the representative P-h curves observed during the nanoindentation test. Each P-h curve has been shifted for clarity of presentation. S1 represents the curve near the center of the impact region, and S6 represents the curve farthest from the impact region. Generally, the plastic deformation of MGs, usually accommodated within narrow shear bands (Greer et al., 2013), is essentially different from that of the crystalline solids. For that, the plastic flow is confined in the tiny space along the indenter tip, and the shear band propagation will be halted once the plastic strain is controlled by the cooperative atomic shear motion in the shear band. Accordingly, the initiation of plastic deformation in MGs during the nanoindentation process is frequently related to a displacement burst or pop-in (Schuh and Nieh, 2003). The representative P-h curves exhibit the emblematic parabolic shape and obvious displacement bursts. It is seen that the P-h curve near the center of shock region shows the ripple-shaped serrations. As the distance from the center of the impact region increases, the pop-in events become stronger and substantially transform into stairstep-like.

To further investigate the evolutionary trend of the serrations, we extracted them from the curves (Liao et al., 2017). The curve of velocity versus time (dh/dt-t) was obtained by differentiating the displacement versus time curve (h-t), as shown in **Figure 4**. It is seen that the serrations correspond to sharp bursts on the dh/dt-t curve, whereas a large number of fluctuations with higher frequencies but smaller amplitudes are also observed, which, nevertheless, come from the noise of the instrument. The
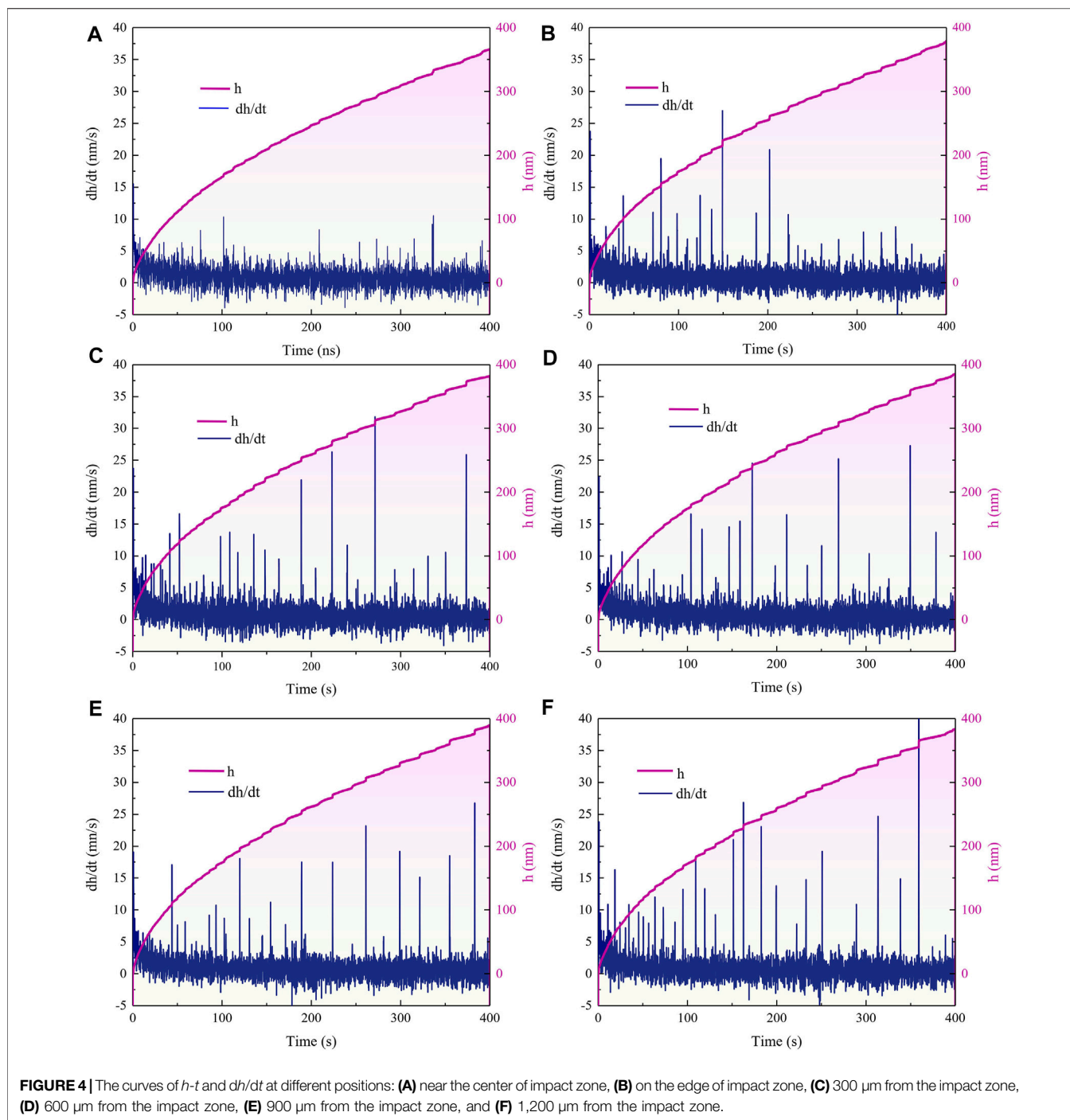
FIGURE 2 | (A) XRD patterns of as-cast and LSP-treated samples. **(B)** The TEM bright field image of LSP-treated sample; the insert is a selected area electron diffraction pattern.

FIGURE 3 | The representative load-displacement (*P-h*) curves from impact region to untreated region.

amplitude of sharp burst is positively correlated with the intensity of serrations. As shown in **Figure 4** A, a small number of low-amplitude sharp bursts is observed, which corresponds to the slight serrations of the *P-h* curve near the center of shock region. The number and amplitude of sharp bursts begin to increase when the indentation position is at the edge of the impact area. Especially, the locations of bursts are mainly concentrated in the first half of the curve. For the unimpacted region, the further the indentation location is from the impact area, the sharper bursts are, and their amplitudes increase steadily. However, this increasing trend gradually weakens as distance increases, and it could be estimated that the number and amplitude of sharp bursts for the *P-h* curve will reach a relatively stable state when

the indentation position is more than a certain distance away from the impact area. Obviously, the evolution in the number and amplitude of sharp bursts reflects the changing mechanical properties of MG induced by LSP. It also indicates that the effect of LSP on MG is not only limited to the impact area but also includes a certain area outside the impact area.

Essentially, the pop-in events are closely related to the localized inhomogeneous plastic flow in MG under loading. More pronounced serrations are associated with more localized plastic flow. In other words, weaker serrations mean better plastic deformation capacity. In this study, the loading rate was kept constant. Thus, it can be expected that the capacity of the plastic flow of MGs is altered by LSP.
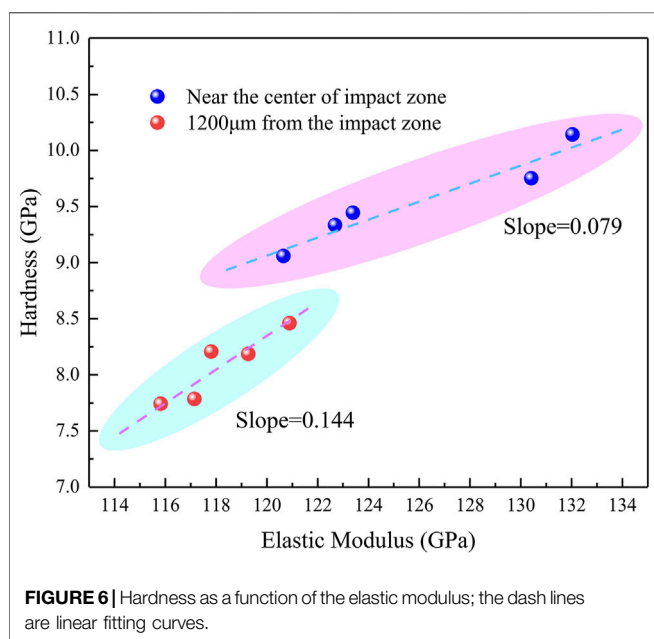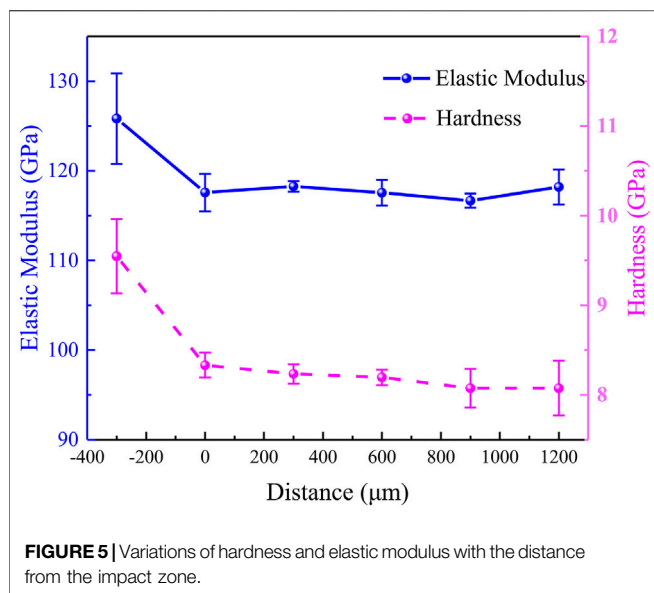
Figure 5 shows the evolution trend of hardness and elastic modulus with increasing distance from the impact point of LSP. Near the center of the shock region, the hardness is higher than that in the untreated zone, exhibiting an apparent work-hardening phenomenon. As the distance increases, the hardness decreases rapidly until the edge of the shock region. Then, it reaches a kind of relative stability outside the impact zone, which means the hardness value fluctuates within a limit range as the distance increases. For the elastic modulus, it also displays a higher value near the center of impact zone and then decreases quickly to the edge of shock region, which is similar to the trend of the hardness. In particular, it is noticeable that the elastic modulus decreases continuously as far away from the impact zone, but this decline in elastic modulus is rather slow and gradually disappears. The evolution of hardness and elastic modulus with distance implies a significant effect of LSP on MG. This effect is affected by the pressure of LSP. In fact, the laser-induced impact pressure induced by LSP in the impact region is not evenly distributed but approximately with a Gaussian distribution, which means that the pressure value is lower in the impact edge region. The evolution of

FIGURE 4 | The curves of *h-t* and d*h*/d*t* at different positions: **(A)** near the center of impact zone, **(B)** on the edge of impact zone, **(C)** 300 μm from the impact zone, **(D)** 600 μm from the impact zone, **(E)** 900 μm from the impact zone, and **(F)** 1,200 μm from the impact zone.

hardness and elastic modulus in the impact region provides evidence of the non-uniform distribution of shock pressure. In addition, the variation of elastic modulus demonstrates that the effect of LSP on MG still exists in a limited range outside the impact zone once again.

Because the indentation hardness and elastic modulus are important parameters for evaluating elastoplastic deformation and plastic flow of structural materials, the relationship between them is of great significance for material application. The

indentation hardness is usually defined as the material under the head average pressure of material resistant to permanent indentation. The elastic modulus is determined by the net force of the bonds between the constituent atoms and the bonds. The resultant force depends on the distance between the atoms. Statistically, the indentation hardness is a function of the elastic modulus of the structure. The ratio of hardness to elastic modulus is the key condition for reflecting the energy dissipation capacity of a material during plastic deformation. The

FIGURE 5 | Variations of hardness and elastic modulus with the distance from the impact zone.

FIGURE 6 | Hardness as a function of the elastic modulus; the dash lines are linear fitting curves.

DISCUSSION

In general, the shock pressure propagates in the form of wave inside the target during the process of LSP. When the shock wave penetrates the target and diffuses quickly, the compressive residual stresses are generated, which is the main reason for the hardness to increase in the impact region. In addition, the shock wave will also reduce the distance between atoms. Because the elastic modulus reflects the binding force between atoms, that is, the larger average atomic distance with decreasing elastic modulus. Conversely, the elastic modulus will rise. It is, therefore, evident that the causal role of shock wave in the alteration of the elastic modulus. It is expected that more energy will be consumed when deformation occurs in impact region, that is, the enhanced energy dissipation capacity of MG. Especially, the above results show that the elastic modulus still decreases slightly in the non-impact zone. It seems possible that these results can be attributed to the edge wave caused by the discontinuous deformation between the impacted and unimpacted regions (Fabbro et al., 1998). However, because of the lower intensity of the edge wave, its effect on material properties is limited.

In addition, the P-h curves have identified the weakening effect of shock wave on pop-in events, that is, the LSP improves the plastic flow capacity of MG. Generally, free volume is the dominant factor for the weakened serrations in P-h curve. The increased free volume reduces the generation of shear bands during the process of indentation, resulting in a weakened serrations phenomenon. However, this explanation fails to interpret the results in this study or even completely contradicts them. The higher hardness and elastic modulus indicate a decrease in free volume content in the shock region (or hardened layer). A possible explanation for this might be that a larger range of cooperative flow of atoms occurs after LSP during indentation. That means, although LSP decreases the content of free volume, the "weak spots" (Antonaglia et al., 2014) that detonate the shear band are also reduced, and the deformation tends to be more holistic.

SUMMARY

In this paper, the micromechanical properties of Zr-based MG after LSP treatment were studied. First, the result of TEM identified that no crystalline grain was generated during LSP. Furthermore, a nanoindentation test was performed to investigate the micromechanical property evolution of Zr-based MG. The representative P-h curves near the center of the shock region exhibited ripple-shaped serrations; the serrations were gradually transformed into stairstep-like for the P-h curves of the region away from the impact region. That means the plastic deformation capacity in shock region was enhanced by LSP. Then, the microhardness and elastic modulus in and around the impact zone were also analyzed. Significant hardening and an increase in elastic modulus were observed in the impact zone, which can be attributed to the effect of compressive residual stress and shock wave. The improvement of hardness

energy dissipation capacity is negatively correlated with this ratio (Bao et al., 2004). In this study, the relationship between hardness and elastic modulus is also investigated. **Figure 6** shows the proportional relationships of hardness and elastic modulus at different regions. The ratio is 0.144 for the region at a distance of 1,200 μm away from impact zone. According to previous results, the effect of LSP on MG is negligible or even invalid at this region, which can represent the intrinsic characteristics of the matrix. Nevertheless, the ratio for the region near the center of impact zone is 0.079, demonstrating that the energy dissipation capacity of MG in this region is enhanced by LSP.

and plastic deformation ability in shock region indicate the excellent effect of LSP on the improvement of micromechanical properties of Zr-based MG. An implication of this is the possibility that the shock wave reduces the existence of "weak spots" in the hardening zone and makes the distribution of atoms more compact and uniform.

DATA AVAILABILITY STATEMENT

The original contributions presented in the study are included in the article/supplementary material; further inquiries can be directed to the corresponding authors.

REFERENCES

Antonaglia, J., Xie, X., Schwarz, G., Wraith, M., Qiao, J., Zhang, Y., et al. (2014). Tuned Critical Avalanche Scaling in Bulk Metallic Glasses. *Sci. Rep.* 4 (1), 1–5. doi:10.1038/srep04382

Argon, A. S. (1979). Plastic Deformation in Metallic Glasses. *Acta Metallurgica* 27 (1), 47–58. doi:10.1016/0001-6160(79)90055-5

Bao, Y. W., Wang, W., and Zhou, Y. C. (2004). Investigation of the Relationship between Elastic Modulus and Hardness Based on Depth-Sensing Indentation Measurements. *Acta Materialia* 52 (18), 5397–5404. doi:10.1016/j.actamat.2004.08.002

Di, S., Wang, Q., Zhou, J., Shen, Y., Li, J., Zhu, M., et al. (2020). Enhancement of Plasticity for FeCoBSiNb Bulk Metallic Glass with Superhigh Strength through Cryogenic thermal Cycling. *Scripta Materialia* 187, 13–18. doi:10.1016/j.scriptamat.2020.05.059

Fabbro, R., Peyre, P., Berthe, L., and Scherpereel, X. (1998). Physics and Applications of Laser-Shock Processing. *J. Laser Appl.* 10 (6), 265–279. doi:10.2351/1.521861

Greer, A. L., Cheng, Y. Q., and Ma, E. (2013). Shear Bands in Metallic Glasses. *Mater. Sci. Eng. R: Rep.* 74 (4), 71–132. doi:10.1016/j.mser.2013.04.001

Greer, A. L., and Ma, E. (2007). Bulk Metallic Glasses: at the Cutting Edge of Metals Research. *MRS Bull.* 32 (8), 611–619. doi:10.1557/mrs2007.121

Huang, H., Zhang, J., Shek, C.-H., and Yan, J. (2016). Effects of Pre-compression Deformation on Nanoindentation Response of $Zr_{65}Cu_{15}Al_{10}Ni_{10}$ Bulk Metallic Glass. *J. Alloys Compd.* 674, 223–228. doi:10.1016/j.jallcom.2016.03.057

Inoue, A. (2000). Stabilization of Metallic Supercooled Liquid and Bulk Amorphous Alloys. *Acta Materialia* 48 (1), 279–306. doi:10.1016/S1359-6454(99)00300-6

Li, Y., Wei, Y., Zhang, K., Zhang, Y., Wang, Y., Tang, W., et al. (2019). Rejuvenation, Embryonic Shear Bands and Improved Tensile Plasticity of Metallic Glasses by Nanosecond Laser Shock Wave. *J. Non-Crystalline Sol.* 513, 76–83. doi:10.1016/j.jnoncrysol.2019.02.031

Liao, G., Long, Z., Zhao, M., Zhong, M., Liu, W., and Chai, W. (2017). Serrated Flow Behavior in a Pd-Based Bulk Metallic Glass under Nanoindentation. *J. Non-Crystalline Sol.* 460, 47–53. doi:10.1016/j.jnoncrysol.2017.01.010

Liao, Y., Ye, C., and Cheng, G. J. (2016). [INVITED] A Review: Warm Laser Shock Peening and Related Laser Processing Technique. *Opt. Laser Technol.* 78, 15–24. doi:10.1016/j.optlastec.2015.09.014

Liu, M., Hou, D., and Gao, C. (2021). Berkovich Nanoindentation of $Zr_{55}Cu_{30}Al_{10}Ni_5$ Bulk Metallic Glass at a Constant Loading Rate. *J. Non-Crystalline Sol.* 561, 120750. doi:10.1016/j.jnoncrysol.2021.120750

Lu, Z., Jiao, W., Wang, W. H., and Bai, H. Y. (2014). Flow Unit Perspective on Room Temperature Homogeneous Plastic Deformation in Metallic Glasses. *Phys. Rev. Lett.* 113 (4), 045501. doi:10.1103/PhysRevLett.113.045501

Miracle, D. B. (2004). A Structural Model for Metallic Glasses. *Nat. Mater* 3 (10), 697–702. doi:10.1038/nmat1219

Montross, C., Wei, T., Ye, L., Clark, G., and Mai, Y. W. (2002). Laser Shock Processing and its Effects on Microstructure and Properties of Metal Alloys: a Review. *Int. J. Fatigue* 24 (10), 1021–1036. doi:10.1016/S0142-1123(02)00022-1

AUTHOR CONTRIBUTIONS

All authors listed have made a substantial, direct, and intellectual contribution to the work and approved it for publication.

FUNDING

Schuh, C. A., and Nieh, T. G. (2003). A Nanoindentation Study of Serrated Flow in Bulk Metallic Glasses. *Acta Materialia* 51 (1), 87–99. doi:10.1016/S1359-6454(02)00303-8

Spaepen, F. (1977). A Microscopic Mechanism for Steady State Inhomogeneous Flow in Metallic Glasses. *Acta Metallurgica* 25 (4), 407–415. doi:10.1016/0001-6160(77)90232-2

Wang, W. H., Dong, C., and Shek, C. H. (2004). Bulk Metallic Glasses. *Mater. Sci. Eng. R: Rep.* 44 (2-3), 45–89. doi:10.1016/j.mser.2004.03.001

Wang, Z., Sun, B. A., Bai, H. Y., and Wang, W. H. (2014). Evolution of Hidden Localized Flow during Glass-To-Liquid Transition in Metallic Glass. *Nat. Commun.* 5 (1), 1–7. doi:10.1038/ncomms6823

Wei, Y., Xu, G., Zhang, K., Yang, Z., Guo, Y., Huang, C., et al. (2017). Anomalous Shear Band Characteristics and Extra-deep Shock-Affected Zone in Zr-Based Bulk Metallic Glass Treated with Nanosecond Laser Peening. *Sci. Rep.* 7 (1), 1–7. doi:10.1038/srep43948

Xie, S., and Kruzic, J. J. (2017). Cold Rolling Improves the Fracture Toughness of a Zr-Based Bulk Metallic Glass. *J. Alloys Compd.* 694, 1109–1120. doi:10.1016/j.jallcom.2016.10.134

Xu, G. Y., Wei, Y. P., and Wei, B. C. (2014). Deformation Feature and Properties of Zr Based Bulk Metallic Glass Treated by Laser Shock Peening. *Mater. Res. Innov.* 18, S4–S798. doi:10.1179/1432891714Z.000000000783

Ye, J. C., Lu, J., Liu, C. T., Wang, Q., and Yang, Y. (2010). Atomistic Free-Volume Zones and Inelastic Deformation of Metallic Glasses. *Nat. Mater* 9 (8), 619–623. doi:10.1038/nmat2802

Zhai, S., Axinte, E., Wang, S., Wang, W., Xing, Q., and Wang, Y. (2018). Effects of Pre-compression on the Microstructure, Mechanical Properties and Corrosion Resistance of $Cu_{47.5}Zr_{47.5}Al_5$ Bulk Metallic Glasses. *J. Non-Crystalline Sol.* 481, 383–390. doi:10.1016/j.jnoncrysol.2017.11.020